Optical Engineering

SPIEDigitalLibrary.org/oe

Calibration technology in application of robot-laser scanning system

YongJie Ren
ShiBin Yin
JiGui Zhu

Calibration technology in application of robot-laser scanning system

YongJie Ren
ShiBin Yin
JiGui Zhu
Tianjin University
State Key Laboratory of Precision Measuring Technology and Instruments
Tianjin 300072, China
E-mail: shibinyin_1987@163.com

Abstract. A system composed of laser sensor and 6-DOF industrial robot is proposed to obtain complete three-dimensional (3-D) information of the object surface. Suitable for the different combining ways of laser sensor and robot, a new method to calibrate the position and pose between sensor and robot is presented. By using a standard sphere with known radius as a reference tool, the rotation and translation matrices between the laser sensor and robot are computed, respectively in two steps, so that many unstable factors introduced in conventional optimization methods can be avoided. The experimental results show that the accuracy of the proposed calibration method can be achieved up to 0.062 mm. The calibration method is also implemented into the automated robot scanning system to reconstruct a car door panel. [DOI: 10.1117/1.OE.51.11.114204]

Subject terms: laser scanner; a fixed sphere; position and pose relationship; two-step method.

Paper 120735 received May 22, 2012; revised manuscript received Oct. 2, 2012; accepted for publication Oct. 15, 2012; published online Nov. 3, 2012.

1 Introduction

As modern industry develops, diversification of products arises and our life improves. How to get the information on objects and their outlines is becoming a new focus in the measurement field. Because the surfaces of many objects are complex and irregular, conventional contact measurements are out of demand. Taking advantage of high measurement speed, significant measurement efficiency, ease of automation, and good flexibility, noncontacting measurement has been widely used in surface outline, reverse engineering,[1] industry vision detecting,[2] and many other tasks.

The portable 3-D scanning system developed rapidly in recent years. It is combined with mechanical equipment such as a robot, coordinate measuring machine (CMM), and turntable, respectively to compose a measurement system with multiple angles and directions to get the whole information of the 3-D object surface. Proposed by literature,[3] a 3-D surface measurement system consisting of robots, turntable, and structural light sensor is studied, and its main purpose is to program the scanning path automatically. The system in our work is similar to the one discussed in literature[3] except for the turntable. Additionally, the calibration technology, which is one of the key tasks in data collection, is significantly explored.

Traditional calibration methods use extra 3-D measuring tools to get the relationship between sensor and robot terminal, such as one-step method proposed by Zhuang.[4] This method needs to estimate some system parameters with the help of other tools, and the estimated value must be accurate, thus, it is inconvenient for the operation. The traditional methods have to solve a homogeneous equation $AX = XB$ or $AX = YB$, and several linear[4–7] and nonlinear solutions[8,9] were reported in literature to solve for X or Y.

Since the methods used in hand-eye calibration of cameras are not suitable for hand-eye calibration of displacement sensors,[10,11] the hand-eye calibration methods with a binocular vision sensor and cone-shaped light are developed by Refs. 12 and 13, respectively.

In terms of the two different combining ways of laser sensor and robot, we proposed a new approach to determine the position and orientation relationship between sensor and robot. Using a standard sphere with known radius as a calibration target, this method can restore the sphere center by fitting multiple circles with scanning data, one for each scanning line, and calibrate the position and orientation relationship between sensor and robot in two steps. Errors resulting from the robot's low precision in positioning can be avoided, and the iterative solution for the hand-eye calibration matrix is not necessary in the process; therefore, the reliability increases.

The paper contains the following sections: The whole measuring system and associated coordinate system are defined in Sec. 2. In Sec. 3 hand-eye calibration methods of the two different combining ways are introduced. Experiments and analysis of hand-eye calibration, and applications of the measuring system are detailed in Sec. 4. Our work is concluded in Sec. 5.

2 System Components

The system consists of a 6-DOF industrial robot, laser sensor, and robot end execution tool (the sensor is fixed on the robot end flange plate or the processing worktable). The robot is connected with the computer by a serial port, and the sensor is connected to the computer via universal serial bus (USB).

The base coordinate system $O_bX_bY_bZ_b$ of the scanning system, in which the sensor is fixed at the end of the robot, is presented in Fig. 1. All measured data are converted to this coordinate system. The end-effector coordinate system is indicated as $O_tX_tY_tZ_t$, the coordinate system origin is

0091-3286/2012/$25.00

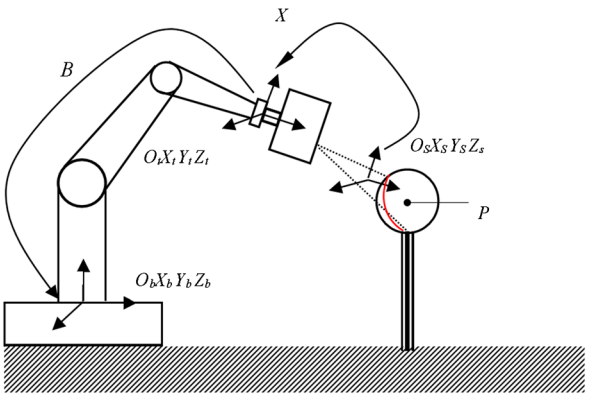

Fig. 1 Flexible measurement system based on robot.

located in the center of the end flange plate, the direction of the X-axis is opposite to the direction of the identify hole on the end flange plate, the Z-axis is perpendicular to the end-effector, and the Y-axis is established as right-handed rule. The laser sensor coordinate system $O_sX_sY_sZ_s$ is located on the laser plane; its X-axis is perpendicular to the laser plane. The tool placed at the end flange plate needs tool coordinate system to define its center point (TCP). Tool coordinate system is defined based on the end-effector coordinate system, which can be used to describe the motion of the robot along its axes. If a tool is worn or replaced, it only needs to redefine the tool coordinate system without any change of the program.

3 Calibrating the Pose Between Robot and Laser Sensor Under Two Combining Ways

The 3-D surface measuring system based on the industrial robot has two combining ways. One method is that the robot moves with the 3-D scanner at its end so that the scanner will reach more positions in the space. The other is that the robot moves with the object to be scanned at its end so that every point of the object can be scanned by the fixed scanner. In either case, the problem that must be solved is how to calibrate the relationship between the scanner's coordinate system and the robot's end-effector coordinate system, i.e., the hand-eye relationship.

3.1 *Laser Sensor Fixed on Robot End*

In this method, hand-eye calibration is to determine the rotation matrix R_S and translation T_S between the laser sensor and robot. We use the hole or sphere as reference through measuring a fixed point at different poses by a robot scanning system. Matrices R_S and T_S can be solved through constraint of the fixed space point. Due to errors of the robot itself, it is difficult to achieve high accuracy, and two-step method described below is proposed.

3.1.1 *Solving the rotation matrix R_S*

For a fixed point in the robot base coordinate system, the relationship between coordinate (x_w, y_w, z_w) in the robot base coordinate system and coordinate (x_s, y_s, z_s) in the laser sensor coordinate system is as follows:

$$\begin{bmatrix} X_W \\ 1 \end{bmatrix} = \begin{bmatrix} R_0 & T_0 \\ 0 & 1 \end{bmatrix} \cdot \begin{bmatrix} R_S & T_S \\ 0 & 1 \end{bmatrix} \cdot \begin{bmatrix} X_S \\ 1 \end{bmatrix}, \tag{1}$$

where X_W is the fixed point's coordinate (x_w, y_w, z_w) in the robot base coordinate system,X_S is the fixed point's coordinate (x_s, y_s, z_s) in the laser scanning sensor coordinate system. R_0 and T_0 are the rotation matrix and translation from $O_tX_tY_tZ_t$ to $O_bX_bY_bZ_b$. R_S and T_S are the rotation matrix and translation from $O_sX_sY_sZ_s$ to $O_tX_tY_tZ_t$. Equation (1) is expanded as follows:

$$X_W = R_0 \cdot R_S \cdot X_S + R_0 \cdot T_S + T_0. \tag{2}$$

Controlling the robot and making the laser sensor measure the same fixed point twice, we obtain the following equations:

$$\begin{cases} X_W = R_{01} \cdot R_S \cdot X_{S1} + R_{01} \cdot T_S + T_{01} \\ X_W = R_{02} \cdot R_S \cdot X_{S2} + R_{02} \cdot T_S + T_{02} \end{cases}. \tag{3}$$

Because the pose of the robot remains unchanged during scanning (the motion with translation only), that is, $R_{01} = R_{02} = R_0$, we can get from Eq. (3)

$$R_0 \cdot R_S \cdot (X_{S1} - X_{S2}) + T_{01} - T_{02} = 0. \tag{4}$$

Here, R_0 is an orthogonal matrix. Collecting several sets of experimental data, we have

$$\begin{aligned} &R_S[X_{S1} - X_{S2} \quad X_{S2} - X_{S3} \quad \ldots \quad X_{S1} - X_{Sn}] \\ &= R_0^T[T_{02} - T_{01} \quad T_{03} - T_{01} \quad \ldots \quad T_{0n} - T_{01}]. \end{aligned} \tag{5}$$

Making $A = [X_{S1} - X_{S2} \;\; X_{S1} - X_{S3} \;\; \ldots \;\; X_{S1} - X_{Sn}]$, $b = R_0^T[T_{02} - T_{01} \;\; T_{03} - T_{01} \;\; \ldots \;\; T_{0n} - T_{01}]$, Eq. (5) can be written as $R_SA = b$. We can use singular value decomposition method to solve this equation, that is,

$$R_S = VU^T. \tag{6}$$

Here, V, U is right singular matrix and left singular matrix of Ab^T.

Note that

$$R_S = \begin{bmatrix} r_1 & r_2 & r_3 \\ r_4 & r_5 & r_6 \\ r_7 & r_8 & r_9 \end{bmatrix}$$

is a rotation matrix and meets the following orthogonal constraints:

$$\begin{aligned} &r_1^2 + r_2^2 + r_3^2 = 1 \\ &r_4^2 + r_5^2 + r_6^2 = 1 \\ &r_7^2 + r_8^2 + r_9^2 = 1 \\ &r_1 \cdot r_4 + r_2 \cdot r_5 + r_3 \cdot r_6 = 0 \\ &r_1 \cdot r_7 + r_2 \cdot r_8 + r_3 \cdot r_9 = 0 \\ &r_4 \cdot r_7 + r_5 \cdot r_8 + r_6 \cdot r_9 = 0. \end{aligned}$$

Therefore, R_S only has three degrees of freedom. During the experiment, the sensor driven by the robot scans the

standard sphere and obtains the centers of the several sections. R_S is solved via Eq. (6).

3.1.2 *Solving the translation T_S*

Using translation motion to scan a fixed sphere, with the coordinates of the laser sensor in $O_sX_sY_sZ_s$ and Eq. (2), the coordinates under $O_bX_bY_bZ_b$ can be acquired, for two different points, we have

$$\begin{cases} X_{W1} = R_{01} \cdot R_S \cdot X_{S1} + R_{01} \cdot T_S + T_{01} \\ X_{W2} = R_{02} \cdot R_S \cdot X_{S2} + R_{02} \cdot T_S + T_{02} \end{cases}. \tag{7}$$

Because the robot is only moved via translation, i.e., $R_{01} = R_{02} = R_0$, Eq. (7) can be simplified as follows:

$$X_{W1} - X_{W2} = R_0 \cdot R_S \cdot (X_{S1} - X_{S2}) + T_{01} - T_{02}. \tag{8}$$

From Eq. (8), the coordinate differences are only related to R_S. If all points are on the fixed sphere, making $T_S = 0$ (T_S can be any constant value; zero is used just for simplification), X_{wi} $(i = 1, 2, 3, \ldots)$ will meet the sphere constraint equation. The fitted center of sphere X_B from X_{wi} and the real center of sphere X_b satisfy the following equation:

$$X_b = X_B + R_0 \cdot T_S, \tag{9}$$

where X_B is the virtual fitting center of the sphere using forward solving at the condition $T_S = 0$, X_b is the real center of the sphere.

Changing the robot's pose and getting another set of X_B and R_0, we have

$$X_b = X_{B1} + R_{01} \cdot T_S \quad X_b = X_{B2} + R_{02} \cdot T_S. \tag{10}$$

From Eq. (10), we further have

$$(R_{02} - R_{01}) \cdot T_S = X_{B1} - X_{B2}. \tag{11}$$

Gathering several sets of experimental data, a linear equation is obtained in the form of matrix: $AT_S = b$, where $A = R_{02} - R_{01}$, $b = X_{B1} - X_{B2}$. Least square method can be easily used to solve T_S:

$$T_S = (A^{\mathrm{T}}A)^{-1}A^T b. \tag{12}$$

3.2 *Laser Scanning Sensor Fixed on a Certain Point in Space*

Under this circumstance, hand-eye calibration is to determine the rotation matrix R_S and translation T_S between the laser sensor coordinate system and robot base coordinate system.

3.2.1 *Solving the rotation matrix R_S*

For a fixed point in the tool coordinate system, the relationship between coordinate (x_t, y_t, z_t) in the tool coordinate system and coordinate (x_s, y_s, z_s) in the laser sensor coordinate system is as follows:

$$\begin{bmatrix} X_t \\ 1 \end{bmatrix} = \begin{bmatrix} R_0 & T_0 \\ 0 & 1 \end{bmatrix}^{-1} \cdot \begin{bmatrix} R_S & T_S \\ 0 & 1 \end{bmatrix} \cdot \begin{bmatrix} X_S \\ 1 \end{bmatrix}, \tag{13}$$

where X_t is the fixed point's coordinate (x_t, y_t, z_t) in the tool coordinate system, X_S is the fixed point's coordinate (x_s, y_s, z_s) in the laser sensor coordinate system. R_0 and T_0 are the rotation matrix and translation from the tool coordinate system to $O_bX_bY_bZ_b$. R_S and T_S are the rotation matrix and translation from $O_sX_sY_sZ_s$ to $O_bX_bY_bZ_b$.

Rewriting Eq. (13),

$$R_0 \cdot X_t + T_0 = R_S \cdot X_S + T_S. \tag{14}$$

Controlling the robot and making the laser sensor measure the same fixed point twice, we obtain the following equation:

$$\begin{cases} R_{01} \cdot X_t + T_{01} = R_S \cdot X_{S1} + T_S \\ R_{02} \cdot X_t + T_{02} = R_S \cdot X_{S2} + T_S \end{cases}. \tag{15}$$

If the pose of the robot remains the same during the scanning process (translation only), that is, $R_{01} = R_{02} = R_0$, we simplify Eq. (15) as

$$T_{01} - T_{02} = R_S \cdot (X_{S1} - X_{S2}). \tag{16}$$

The standard sphere is mounted on the robot. Collecting several sets of experimental data, the steps to solving R_S are similar to those in Sec. 3.1.

3.2.2 *Solving the translation matrix T_S*

From Eq. (14), we have

$$X_t = R_0^{-1} \cdot (R_S \cdot X_S + T_S - T_0) = R_0^{-1} \cdot (R_S \cdot X_S - T_0) + R_0^{-1} \cdot T_S. \tag{17}$$

Using translation motion to scan a fixed sphere, with the coordinates in $O_sX_sY_sZ_s$ and Eq. (17), for two different space points X_{t1}, X_{t2}, we have

$$\begin{cases} X_{t1} = R_{01}^{-1} \cdot (R_S \cdot X_{S1} - T_{01}) + R_{01}^{-1} \cdot T_S \\ X_{t2} = R_{02}^{-1} \cdot (R_S \cdot X_{S2} - T_{02}) + R_{02}^{-1} \cdot T_S \end{cases}. \tag{18}$$

Because robot only has translational motion, that is, $R_{01} = R_{02} = R_0$, Eq. (18) can be simplified as follows:

$$X_{t1} - X_{t2} = R_{01}^{-1} \cdot R_S \cdot (X_{S1} - X_{S2}) + R_{01}^{-1}(T_{01} - T_{02}). \tag{19}$$

From Eq. (19), the coordinate differences are only related to R_S. If all points are on the fixed sphere, making $T_S = 0$, X_{ti} $(i = 1, 2, 3 \ldots)$ will meet the sphere constraint equation, the fitted center of sphere X_B and the real center of sphere X_b satisfy

$$X_b = X_B + R_0^{-1} \cdot T_S. \tag{20}$$

Changing the robot's pose and gathering several sets of experimental data, T_S can be solved. The procedures to get T_S are similar to those in Sec. 3.1.

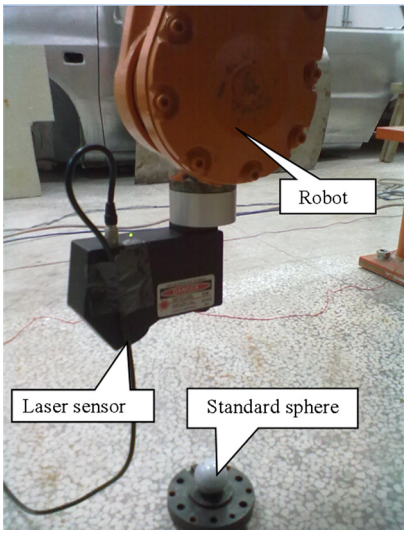

Fig. 2 Calibration setup of the robot-laser scanning system.

4 Calibration Experiment and Application of Robot-Laser Scanning System

4.1 *Experiment Equipment and Pose Calibration*

The measuring system is built based on the first method shown in Fig. 2. It mainly consists of an nxSensor-I 3-D laser sensor made by NextWare. Inc and an ABB IRB2400 robot. The laser sensor is mounted on the robot by a connecting rod. With high integration of state-of-the-art laser technology, electronic imaging, and a digital signal processor (DSP), the nxSensor-I 3-D laser sensor simultaneously possesses qualities of high speed, excellent accuracy, and portability. The specifications of nxSensor-I and the calibration target are as follows:

- Measuring range: $-60\ \text{mm}(z) \times 48\ \text{mm}(y)$ (far end) $\sim +40\ \text{mm}(z) \times 28\ \text{mm}(y)$ (near end)
- Resolution: 5 μm
- Accuracy: up to 25 μm
- Radius of sphere: 19.1 mm.

A standard sphere is used as a calibration target and placed within the range of the robot and laser sensor. First, the laser sensor scans the standard sphere. By fitting circles with the section data, the center coordinates of the sphere under $O_sX_sY_sZ_s$ can be calculated. Since the center coordinates of the sphere may have two solutions from one section, the true value is determined through the position of the scan line on the sphere. R_0 and T_0 are read from the robot control system. The robot moves with only translation, and the sphere is scanned in the same way. The value R_0 and T_0 are recorded at each position, and the center coordinates of the sphere under $O_sX_sY_sZ_s$ is computed. Several groups of experimental data are collected. By substituting these data into Eq. (6), R_S is solved.

For example, when the robot is in its first position, the point data from the sensor can be fitted to an arc corresponding to the center of the circle (0.000000, 5.165, −41.423). When scanning, the sensor's light plane and YOZ coordinate plane are coincident so the X coordinates of the point cloud are all zero. With the sphere radius of 19.1, the center coordinates of the sphere are (13.934, 5.615, −41.423) and can be calculated and listed in the first row of Table 1 (xc, yc, zc).

Table 1 lists 10 groups of robot positon coordinates and the fitted sphere center (xc, yc, zc) computed from the scanning point cloud of each robot position. The positon and orientation of the robot are defined by (tx, ty, tz) and $(q1, q2, q3, q4)$, respectively, which can be read from the robot controller.

The pose of the robot in the first four positions remains unchanged during scanning (the motion with translation only).

R_s is computed from the first four groups of data in Table 1:

Table 1 Robot coordinates and fitted sphere centers.

No.	*q*0	*q*1	*q*2	*q*3	*tx*	*ty*	*tz*	*xc*/mm	*yc*/mm	*zc*/mm
1	0.0372	−0.9945	0.0171	−0.0961	891.7	−118.3	1076.6	13.934	5.615	−41.423
2	0.0372	−0.9945	0.0171	−0.0961	891.7	−116.1	1071.1	13.118	4.185	−35.834
3	0.0372	−0.9945	0.0171	−0.0961	891.7	−111.2	1071.1	8.486	3.433	−34.912
4	0.0372	−0.9945	0.0171	−0.0961	891.7	−104.8	1071.1	2.176	2.365	−33.783
5	0.0360	−0.995	0.0164	−0.0960	902.4	−95.6	1071.5	−6.276	11.189	−30.271
6	0.0360	−0.995	0.0164	−0.0960	902.4	−92.2	1065.7	−8.260	9.331	−24.180
7	0.091	−0.722	0.685	−0.0464	913.2	−124.8	1066.3	−3.284	1.020	−28.120
8	0.091	−0.722	0.685	−0.0464	927.9	−124.0	1064.2	10.539	0.811	−22.853
9	0.0593	−0.859	0.236	−0.450	600.2	46.5	908.0	2.0339	−1.722	−46.622
10	0.0593	−0.859	0.236	−0.450	600.2	26.6	908.0	−13.948	10.474	−44.157

$$R_s = \begin{bmatrix} 0.1181 & -0.9924 & -0.0343 \\ -0.9851 & -0.1215 & 0.1219 \\ -0.1252 & 0.0194 & -0.9919 \end{bmatrix}.$$

There are two sets of pose data (the last six groups of data) in Table 1, which are substituted into Eq. (12) to solve T_S as a result:

$$T_s = [1.898 \quad 26.437 \quad 471.026].$$

The standard sphere ($R = 19.1$ mm) is then scanned in a calibrated measurement system. The standard deviation between the point cloud and the fitted sphere is used to evaluate the accuracy of the system. The scanning point cloud of the standard sphere in the robot base coordinate system is shown in Fig. 3. The resulted radius is 19.1346 mm and root mean square (RMS) error is 0.0622 mm, which shows that the implemented calibration method has a higher accuracy.

4.2 *Application*

Based on the calibrated result above, a car door panel is scanned. The scanning setup is shown in Fig. 4. Reduced point cloud and 3-D surface reconstruction are shown in Figs. 5 and 6, respectively. In order to avoid the ripple of the all-angle robot arm, the robot is moved in discrete steps with only one joint while scanning a specific area of the car door. The joint has been moved to the greatest extent to scan a larger area of the car door, which is a flat object. The ripple of the robot is reduced greatly due to this single joint motion pattern, and the precision of registration of the scanning point cloud is improved greatly as well. The registration of the scanning point cloud is based on an iterative closest point (ICP) algorithm,[14,15] which is a level of art registration in data processing of the 3-D laser scanning point cloud.

Scanning with an all-angle robot arm always exhibits ripple, which is a major source of error of the scanning system. In order to avoid the ripple of the all-angle robot arm during scanning objects with big and complex surfaces and improve the accuracy of the system, more significant work is in progress. A precise linear rail is added to the flange end of the robot arm, and the sensor is fixed on the linear rail, as shown in Fig. 7. While scanning, the robot is moved to discrete positions, and the linear rail takes the scanner to perform linear scanning. Through combining the precise linear rail with the industrial robot, the system can get very precise scanning data within the range of the precise linear rail. After registration of the scanning point cloud, a precise whole sense of the scanned object is available.

For comparison, another measuring system is set up, which mainly consists of a Leica AT901 laser tracker and T-Scan. The uncertainty of T-Scan within a range of 5 m is $\pm 95\ \mu\text{m} + 3\ \mu\text{m/m}$ ($k = 2$). A standard plane with an area of about 0.04 m^2 is scanned by both systems, and flatness error is calculated with the scanning data, which is up to 0.0397 mm for T-Scan and 0.0504 mm for the robot-laser scanning system.

Through combining the robot with the laser sensor, the system flexibility is improved greatly, and automated scanning and flexible machining become possible. Using the fixed point constraint and two-step method, key pose relationship among the systems can be solved, and the full 3-D scanning task can be achieved by the robot-sensor system. The technologies implemented in the proposed measuring system can also be used in the field of reverse engineering and robot flexible machining.

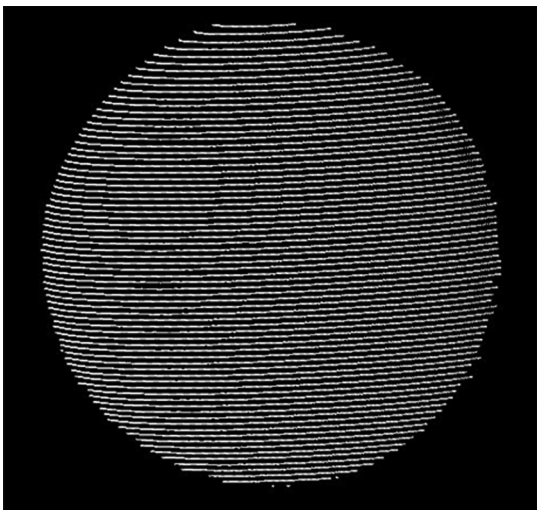

Fig. 3 Point cloud of the sphere.

Fig. 4 Scanning setup of a car door panel.

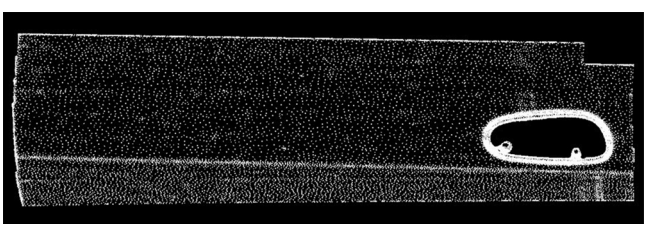

Fig. 5 Reduced point cloud of the car door.

Fig. 6 3-D surface reconstruction of the car door.

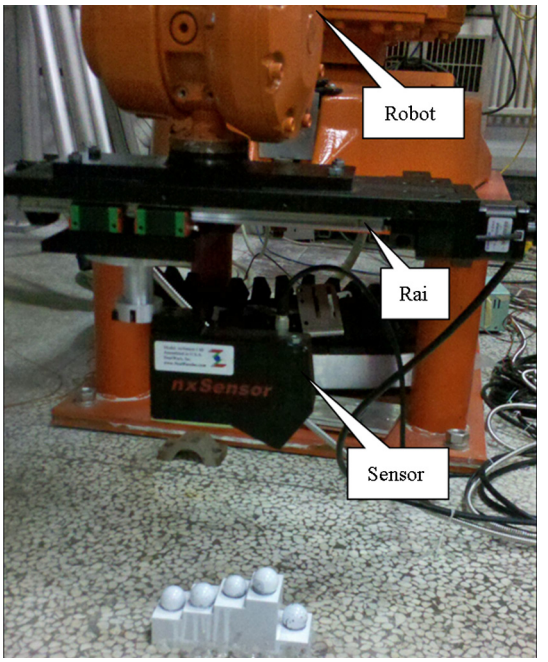

Fig. 7 Scanning system of robot-laser combined with linear rail.

5 Conclusion

The proposed scanning system of robot and laser sensor has expanded the scope of work of the laser scanner to a certain extent and will reduce the labor intensity compared with manual scanning. The presented two-step calibration method can determine the hand-eye relationship between the robot and laser sensor without using iterative optimization. Calibration accuracy is achieved up to 0.062 mm, which has been a challenge in the measurement applications of the robot. The unique contribution of this work is to avoid the angular errors during the calibration, which usually prevent robots from being used in the measuring applications. The experimental results show that high accuracy and good stability can be achieved in such a system, and there is a good application prospect.

References

1. S. Onuh, N. Bennett, and J. Baker, "Rapid prototyping: practical approach to enabling reverse engineering," *Proc. SPIE* **4566**, 145–151 (2001).
2. R. Yang et al., "Robust and accurate surface measurement using structured light, *IEEE Trans. Instrum. Meas.* **57**(6), 1275–1280 (2008).
3. S. Larsson and J. A. P. Kjellander, "An industrial robot and a laser scanner as a flexible solution towards an automatic system for reverse engineering of unknown objects," in *Proc. 7th Biennial Conf. Eng. Syst. Design and Analysis*, pp. 341–350 (2004).
4. H. Zhuang, Z. Roth, and R. Sudhakar, "Simultaneous robot/world and tool/flange calibration by solving homogeneous transformation of the form $AX = YB$," *IEEE Trans. Robot. Autom.* **4**(10), 549–554 (1994).
5. F. Park and B. Martin, "Robot sensor calibration: solving $AX = XB$ on the Euclidean group," *IEEE Trans. Robot. Autom.* **10**(5), 717–721 (1994).
6. R. Y. Tsai and R. K. Lenz, "A new technique for fully autonomous and efficient 3D robotics hand/eye calibration," *IEEE Trans. Robot. Autom.* **5**(3), 345–358 (1989).
7. C.-C. Wang, "Extrinsic calibration of a robot sensor mounted on a robot," *IEEE Trans. Robot. Autom.* **8**(2), 161–175 (1992).
8. R. Horaud and F. Dornaika, "Hand-eye calibration," *Int. J. Robot. Res.* **14**(3), 195–210 (1995).
9. F. Dornaika and R. Horaud, "Simultaneous robot-world and hand-eye calibration," *IEEE Trans. Robot. Autom.* **14**(4), 617–622 (1998).
10. H. Zhuang, K. Wang, and Z. S. Roth, "Simultaneous calibration of a robot and a hand-mounted camera," *IEEE Trans. Robot. Autom.* **11**(5), 649–660 (1998).
11. C. Chen and A. KaK, "Modeling and calibration of a structured light scanner for 3D robot vision," in *Proc. IEEE Int. Conf. Robot Autom.*, pp. 807–815 (1987).
12. H. J. Liu, F. H. Shi, and Y. C. Liu, "Simulation analysis on robotic hand-eye calibration," *J. Syst. Simulation* **16**(11), 2541–2543 (2004).
13. D.-J. Park and J.-H. Kim, "3D hand-eye robot vision system using a cone-shaped structured light," in *Int. Joint Conf. 2006 (SICE-ICCAS 2006)*, Busan, Korea, pp. 2975–2980 (2006).
14. P. J. Besl and N. D. McKay, "A method for registration of 3D shapes," *IEEE Trans. Pattern Anal. Mach. Intell.* **14**(2), 239–256 (1992).
15. G. Blais and M. D. Levine, "Registering multiview range data to create 3D computer graphics," *IEEE Trans. Pattern Anal. Mach. Intell.* **17**(8), 820–824 (1995).

YongJie Ren received his MS and PhD degrees in precision measuring technology and instruments from the University of Tianjin in 2004 and 2007, respectively. From 2007 until now, he has been a lecturer in the Institute of Precision Measuring Technology and Instruments, Tianjin University. His research interests are in photo-electric detection and precision measuring as well as controlling and measuring of industrial robot.

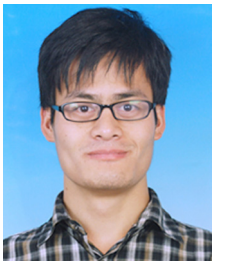

ShiBin Yin is a PhD candidate in precision measuring technology and instruments in University of Tianjin, and he received his MS degree in precision measuring technology and instruments from the University of Tianjin in 2012. His research interests are in photo-electric precision measuring and controlling and measuring of industrial robot.

JiGui Zhu: biography and photograph not available.